Polymer 49 (2008) 2202–2210

Contents lists available at ScienceDirect

Polymer

journal homepage: www.elsevier.com/locate/polymer

Enhancing electrochromic properties of polypyrrole by silsesquioxane nanocages

Metin Ak[a,b], Burcin Gacal[c], Baris Kiskan[c], Yusuf Yagci[c,*], Levent Toppare[a,**]

[a] Middle East Technical University, Department of Chemistry, 06531 Ankara, Turkey
[b] Pamukkale University, Department of Chemistry, 20017 Denizli, Turkey
[c] Istanbul Technical University, Department of Chemistry, Maslak, Istanbul 80626, Turkey

ARTICLE INFO

Article history:
Received 12 November 2007
Received in revised form 1 March 2008
Accepted 12 March 2008
Available online 18 March 2008

Keywords:
Polyhedral oligomeric silsesquioxane
Conducting polymers
Polypyrrole

ABSTRACT

A new monomer, octa(thiophenephenyl)silsesquioxane (O*Thiophene*PS) was synthesized via click chemistry. The chemical structure of O*Thiophene*PS was characterized by nuclear magnetic resonance (^{1}H NMR) and Fourier transform infrared (FT-IR) spectroscopies. Electrochemical polymerization of pyrrole with O*Thiophene*PS was performed resulting in polypyrrole-attached, polyhedral oligomeric silsesquioxane (OPS–PPy). The spectroelectrochemical studies show that the electrochromic properties of (OPS–PPy) are superior to those of polypyrrole (PPy). This great improvement can be attributed to the more accessible doping sites and the facile ion movement during the redox switching brought by the loose packing of the PPy chains.

1. Introduction

Polyhedral oligomeric silsesquioxanes (POSSs) are well-known as novel building blocks for inorganic–organic hybrid materials [1]. POSSs can have an organic substituent on each silicon atom at the corner of the core where the core is based on insulating siloxane bond. Thus, when photo- and electroactive chromophores are introduced as the organic substituents on silicon atom, these chromophores are expected to be isolated from each other by both steric and electronic effects. The isolation of the chromophores will solve the problems due to their aggregation in solid state caused by π–π interactions, such as crystallization and formation of excimers. However, there are few reports on the introduction of photo and electroactive chromophores as the substitutents on silicon atom [2].

Conducting polymers have received significant attention throughout two decades, stemming not only from their high conductivities in the doped state but also from a variety of opto-electronic and redox properties [3]. One of these properties is electrochromism, which is defined as the reversible electromagnetic absorbance/transmittance change in response to an externally applied potential [4]. Several properties, crucial for the success of potential electrochromics (EC) for such device applications as electrochromic windows, mirrors, and displays are embodied by organic polymer systems. These include rapid response times, optical density change, low power requirements, high and efficient color changes in response to applied potentials, and the ability to structurally modify the monomer to achieve specific colors. Electrochromic contrast is one of the most important parameters in evaluating electrochromic materials. Modification of repeat-unit structures of conjugated polymers is the most common strategy for improving the optical contrast.

For poly(3,4-ethylenedioxythiophene) (PEDOT) derivatives, contrast can be improved significantly by attaching additional electrochromic groups as a side pendant group to ethylenedioxy ring [5] or copolymerization with novel monomers [6]. Contrast enhancement can also be achieved by increasing the alkylenedioxy ring size [7] or incorporating rigid/bulky substituents onto the ethylenedioxy ring [8] since the bulky rings or substituents can separate the polymer chains and hence allow facile ion movement during redox switching. Similarly, first generation dendron substituted conducting polymers have also been found to exhibit high electrochromic contrasts owing to their large inter-chain distances [9]. However, existing synthetic approaches for improving the contrast of conjugated polymers have been extensively exploited to manipulate the chemical structures of the monomers. On the other hand, physical approaches, such as making mesoporous electrochromic polymer thin films to facilitate ion diffusion [10] and reducing the diffusion distance for the dopant ions through the use of conjugated polymer nanotubes [11] or porous microspheres [12] had insignificant impacts on the contrast together with considerable improvement on the switching speed of the devices. Another physical approach to

---

* Corresponding author. Tel.: +902122856386; fax: +902122856169.
** Corresponding author. Tel.: +903122103251; fax: +903122103200.
E-mail addresses: yusuf@itu.edu.tr (Y. Yagci), toppare@metu.edu.tr (L. Toppare).

0032-3861/$ – see front matter © 2008 Elsevier Ltd. All rights reserved.
doi:10.1016/j.polymer.2008.03.023

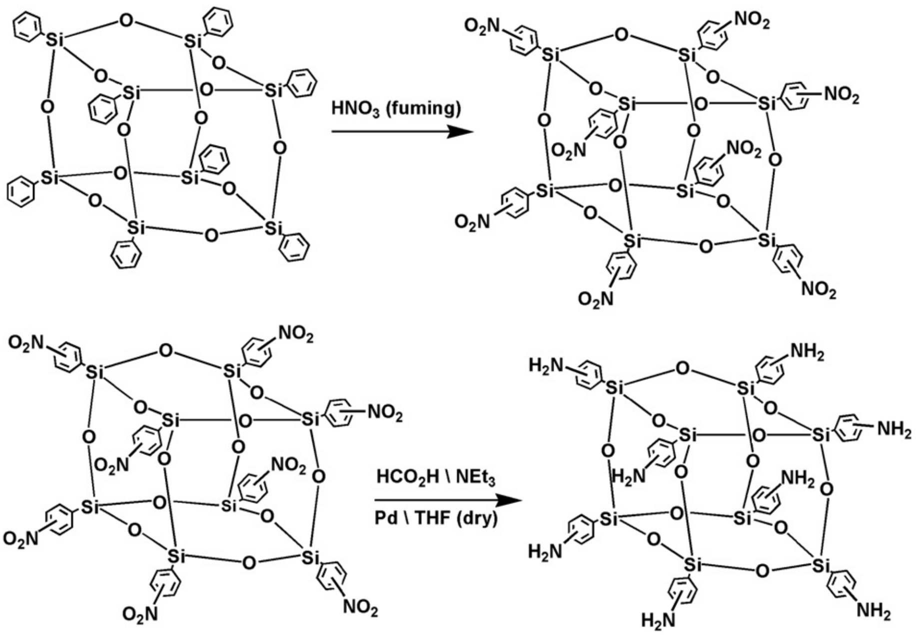

Scheme 1. Synthesis of octa(azidophenyl)silsesquioxane (ON_3PS).

enhance the contrast of the conducting polymer is the electrostatic layer-by-layer assembly technique. This technique has been shown to create low-roughness electroactive polymer films of exceptional homogeneity and high optical contrast [13].

Recently, 1,3-dipolar cycloadditions from the reactions between azides and alkynes or nitriles, known as "click reactions" [14–16], have been recognized as a useful synthetic methodology and have been applied to macromolecular chemistry to offer materials ranging from block copolymers to complex macromolecular structures [17–24]. These cycloaddition reactions enabled the C–C bond formation in a quantitative yield without side reactions which avoids additional purification steps. The click reactions are particularly important in preparative methods, in which high conversion of functional groups is desirable. Numerous applications of click chemistry in polymer science as well as molecular biology and nanoelectronics have recently been reviewed [25,26].

In this study, we introduce a new approach for improving the electrochromic properties of polypyrrole by attaching polypyrrole chains onto thiophene possessing OPS nanocages which are efficiently synthesized via click chemistry. This process prohibits the dense packing of the rigid chains and gives rise to a nanometer-scale porous structure, and hence greatly facilitates ion extraction and injection. With this approach, not only properties of polypyrrole but also other polymers prepared by the copolymerization of functional POSS with the wide variety of monomers may be tuned easily.

2. Experimental

2.1. Materials

Tetrabutylammonium tetrafluoroborate (TBAFB), dichloromethane (DCM), octaphenylsilsesquioxane (OPS, Aldrich), 3-thiophenecarboxylic acid (99%, Acros), propargyl bromide (~80 vol% in toluene, Fluka), tetrabutylammonium bromide (TBAB, Acros Organics 99%), copper(I) bromide ($\geq$97.0%, Riedel-deHaën), 2,2′-bipyridine ($\geq$99%, Aldrich), sodium azide ($\geq$99.0%, Fluka), sodium nitrite ($\geq$99.0% Sigma–Aldrich), sulfuric acid (98%, Sigma–Aldrich), sodium hydroxide ($\geq$97.0%, Sigma–Aldrich), anhydrous magnesium sulfate (99%, Sigma–Aldrich) and ethyl acetate ($\geq$99%, Sigma) were used as received. Pyrrole (Py) was purified by double distillation and tetrahydrofuran (THF, 99.8%, J.T. Baker) was dried and distilled over benzophenone–Na.

2.2. Instruments

^{1}H NMR spectra were recorded in DMSO-d_6 with $Si(CH_3)_4$ as the internal standard, using a Bruker AC250 (250.133 MHz) instrument. FT-IR spectra were recorded on a Perkin–Elmer FTIR Spectrum One spectrometer. A three-electrode cell containing ITO-coated glass slides (Delta Technologies, $R = 8–12\ \Omega\ sq^{-1}$) as the working electrode, a platinum foil as the counter electrode, and a silver wire as the pseudo-reference electrode was used for electrodeposition of polymer films by potentiodynamic methods. All electrochemical work was performed on a Voltalab PST50 potentiostat/galvanostat. Agilent 8453 spectrophotometer was used to perform the spectroelectrochemical studies of the copolymer and the characterization of the devices. Colorimetry measurements were done via Minolta CS-100 spectrophotometer.

2.3. Synthesis of octa(nitrophenyl)silsesquioxane (ONO_2PS)

Octa(nitrophenyl)silsesquioxane was synthesized according to the literature reported by Laine et al. [27]. ^{1}H NMR (DMSO-d_6): 8.8–7.0 (Ar, 4.0H). FT-IR (cm^{-1}): 1527 (νN=O asym.), 1348 (νN=O sym.), 1304–990 (νSi–O–Si).

2.4. Synthesis of octa(aminophenyl)silsesquioxane (ONH_2PS)

Octa(aminophenyl)silsesquioxane was synthesized according to the literature reported by Laine et al [27]. ^{1}H NMR (DMSO-d_6): 7.9–6.1 (Ar, 4.0H), 5.5–4.4 (–N*H*, 2.0H). FT-IR (cm^{-1}): 3368 (νN–H asym.), 3456 (νN–H sym.), 1304–990 (νSi–O–Si).

2.5. Synthesis of octa(azidophenyl)silsesquioxane (ON_3PS)

Water (0.3 ml) was placed in a round-bottomed flask equipped with a thermometer and an efficient mechanical stirrer. While stirring 0.09 mL concentrated sulfuric acid were added, followed by 0.5 g (4.33×10^{-4} mol) ONH_2PS. When all the amine was converted to the brown sulfate, 0.2 mL water were added and the suspension

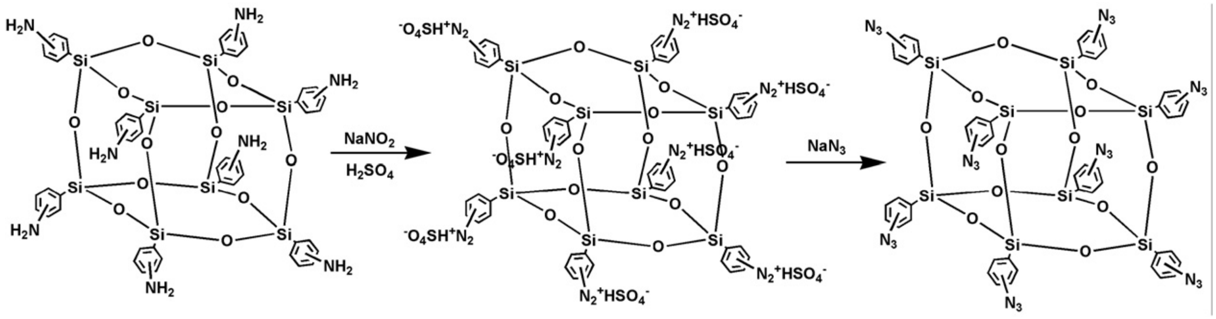

Scheme 2. Synthesis of octa(azidophenyl)silsesquioxane (ON_3PS).

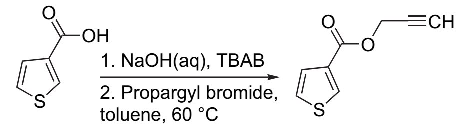

Scheme 3. Synthesis of prop-2-ynyl thiophene-3-carboxylate (*propargyl*thiophene).

was cooled to 0–5 °C in an ice–salt bath. A solution of 0.032 g (4.62×10^{-4} mol) sodium nitrite in 0.2 mL water was added dropwise over a period of 15 min, and the mixture was further stirred for another 45 min. A thick precipitate of the sparingly soluble diazonium salt was separated from the initially clear solution during this period. With vigorous stirring, a solution of 0.03 g (4.91×10^{-4} mol) sodium azide in 0.3 mL of water were added, and stirring was continued for 40 min. The thick dark brown solid was filtered with suction and washed with water. The material was allowed to dry in air in a dark place. ^{1}H NMR (DMSO-d_6): 7.8–6.2 (Ar, 4.0H). FT-IR (cm^{-1}): 2104 (ν–N≡N), 1304–990 (νSi–O–Si). Element. Anal. Calc.: C (42.34%); H (2.37%); found: C (38.89%); H (2.98%).

2.6. Synthesis of prop-2-ynyl thiophene-3-carboxylate (propargyl*thiophene*)

In a 250 mL flask 3-thiophenecarboxylic acid (2.0 g, 15 mmol) was dissolved in 100 mL 0.1 N NaOH. The mixture was heated at 50 °C until a clear solution was formed. To this solution, tetrabutylammonium bromide (0.5 g, 1.55 mmol) was added as a phase transfer catalyst. A solution of propargyl bromide (2.04 g, 17 mmol) in 20 mL toluene was added portion wise to the solution. The mixture was kept stirring at 60 °C for 24 h. Then the toluene layer was separated and washed repeatedly with 2% NaOH (200 mL, 0.1 N) and with water. Evaporating toluene afforded the product. This was washed with cold hexane, and dried under vacuum (yield: ca. 60%). ^{1}H NMR (DMSO-d_6): 8.14 (1.0H), 7.54 (1.0H), 7.33 (1.0H), 4.86 (1.0H), 2.50 (1.0H). FT-IR (cm^{-1}): 3293 (ν≡C–H), 2129 (νC≡C), 1716 (νC=O).

2.7. *General procedure for synthesis of octa(*thiophene*phenyl) silsesquioxane (O*Thiophene*PS) via click chemistry*

Octa(azidophenyl)silsesquioxane (0.20 g, 2.2×10^{-4} mol), prop-2-ynyl thiophene-3-carboxylate (0.04 g, 2.42×10^{-4} mol), CuBr (0.047 g, 3.3×10^{-4} mmol) and 2,2′-bipyridine (0.057 g, 3.63×10^{-4} mmol) were dissolved in 10 mL THF in a schlenk tube. The tube was degassed by three freeze-pump-thaw cycles and left in nitrogen. The reaction was carried out for 41 h at room temperature. The solution was filtered. This solution was put in a separatory funnel with 25 mL dilute H_2SO_4 (aq) solution and 30 mL ethyl acetate. The solution was washed with 150 mL aliquots of dilute acid solution and then with $NaHCO_3$ (aq) solution and finally with water. The organic layer was then dried over $MgSO_4$ to remove water and precipitated by pouring into hexane. The precipitate was collected by filtration. The dark brown powder was vacuum dried. ^{1}H NMR (DMSO-d_6): 8.14 (1.0H), 7.54 (1.0H), 7.33 (1.0H), 4.86 (1.0H), 2.50 (1.0H). FT-IR (cm^{-1}): 1716 (νC=O). Element.Anal. Calc.: C (49.99%); H (3.00%); found: C (48.37%); H (3.60%).

2.8. *Synthesis of PPy and OPS–PPy*

Electrochemical polymerization of OPS–PPy was carried out by sweeping the potential between −0.8 V and +1.1 V with 40 mV/s scan rate in the presence of 50 mg O*Thiophene*PS and 10 μL Py in TBAFB (0.1 M)/DCM electrolyte–solvent couple. The working and counter electrodes were Pt wire and the reference electrode was Ag wire. Experiments were repeated with feed ratios where the amounts of OPS and pyrrole were different. OPS–PPy was washed with DCM in order to remove excess electrolyte and unreacted monomer after the potentiodynamic electrochemical polymerization. PPy was synthesized under the same conditions. For the spectroelectrochemical studies polymers were synthesized in the same solvent–electrolyte couple on an ITO-coated glass slide using a UV-cuvette as a single-compartment cell equipped with Pt counter electrode and Ag wire reference electrode. The electrochromic measurements, spectroelectrochemistry and switching

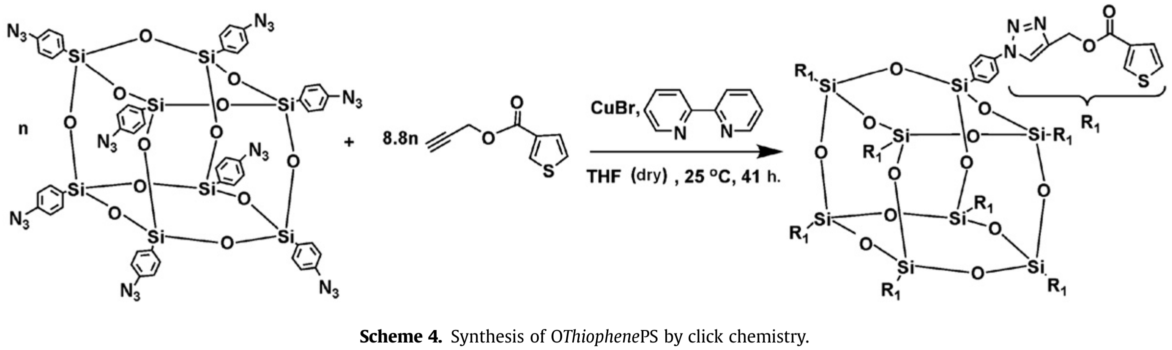

Scheme 4. Synthesis of O*Thiophene*PS by click chemistry.

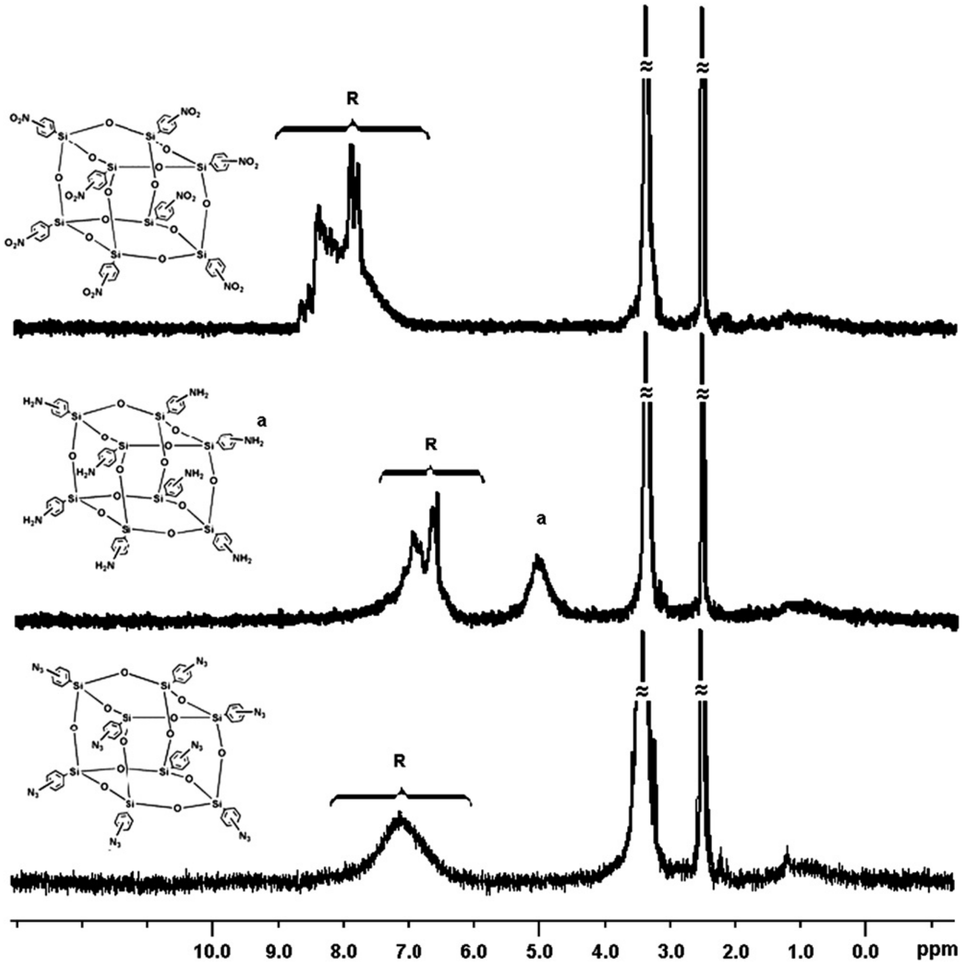

Fig. 1. ^{1}H NMR spectra of ONO_2PS, ONH_2PS and ON_3PS (R: aromatic protons).

studies of the polymer films were carried out in the same media in the absence of monomer.

3. Results and discussion

3.1. Synthesis and characterization

We report here the synthesis of octa(azidophenyl)silsesquioxane (ON_3PS) cube from the corresponding octa(aminophenyl)-silsesquioxane (ON_3PS) via their diazonium salts and the use of "click chemistry" as a facile route for functionalization of octa(phenyl) silsesquioxane (OPS). For this purpose, the octa(nitrophenyl) silsesquioxane (ONO_2PS) was synthesized by a modified literature procedure reported by Laine et al. [27,28]. This improved procedure provides ONO_2PS with one nitro group per phenyl unit. ONO_2PS is quantitatively transformed to ONH_2PS by hydrogen-transfer reduction in the presence of formic acid, triethylamine and Pd/C catalyst (Scheme 1) [27,28].

For the synthesis of parent ON_3PS cube a simple synthetic strategy was used (Scheme 2). The aqueous solution of sodium nitrite in concentrated sulfuric acid (a nitrosonium hydrogen sulfate reagent) is used as a very effective diazotizing medium at 0 °C. The resulting diazonium salt is replaced by azide attached to the aromatic ring by the evolution of molecular nitrogen in quantitative conversion (99–100%).

In this study, propargyl containing thiophene was selected as the electropolymerizable click component which was synthesized via esterification reaction of thiophene-3-carboxylic acid with propargyl bromide (Scheme 3).

Then a standard "click" protocol has been established. The ON_3PS was dissolved in THF and reacted with *propargyl*thiophene in the presence of a catalytic amount of CuBr, and bipyridine at room temperature. The reaction afforded the desired product O*Thiophene*PS (Scheme 4). After removing the catalyst, the O*Thiophene*PS was precipitated and dried under vacuum.

The structures of the intermediates and final product were confirmed by ^{1}H NMR spectra (DMSO-d_6) (Fig. 1). The aromatic

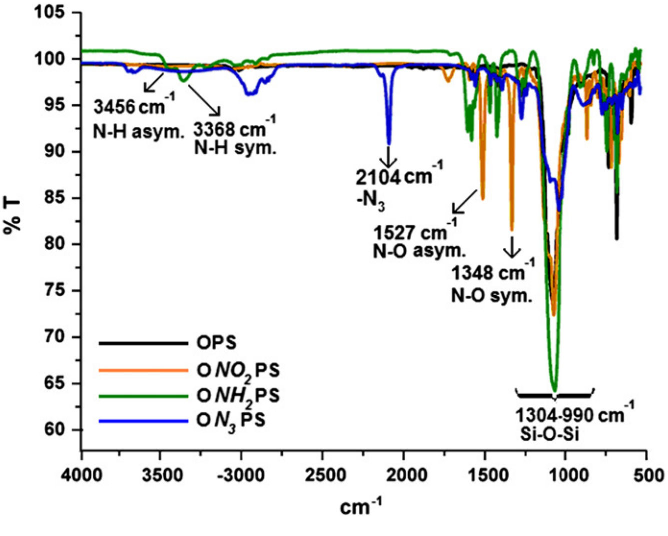

Fig. 2. FT-IR spectra of ONO_2PS, ONH_2PS and ON_3PS.

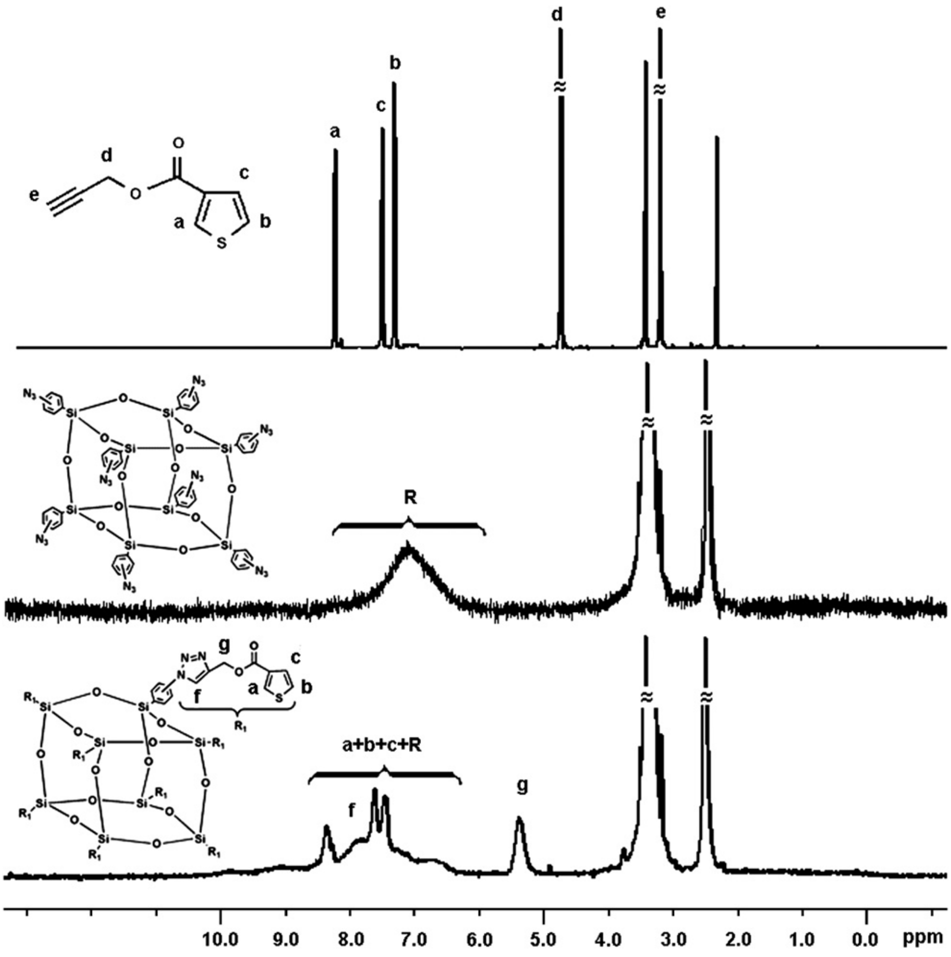

Fig. 3. ^{1}H NMR spectra of *propargyl*thiophene, O*N*$_3$PS and O*Thiophene*PS (R: aromatic protons).

protons of phenyl groups emerge at around 8 ppm, due to the electron withdrawing effect of the –NO$_2$. The reduction process led to two changes in the spectra. While N–H protons appeared at 5.50–4.40 as new peaks, the aromatic peaks appear at higher magnetic fields in the range of 7.9–6.1 ppm. The integration ratios of N–H protons to aromatic C–H protons are 1:2, respectively, indicating quantitative reduction of the nitro groups to amino groups. The efficient transformation of O*NH*$_2$PS to O*N*$_3$PS was also evidenced from ^{1}H NMR spectrum wherein the resonance due to N–H protons disappeared completely.

Additionally, FT-IR spectra of the related compounds confirm the NMR data. O*NO*$_2$PS exhibits strong symmetric and asymmetric νN═O peaks at 1348 and 1527 cm^{-1} (Fig. 2). These peaks disappear completely after reduction and new broad symmetric and

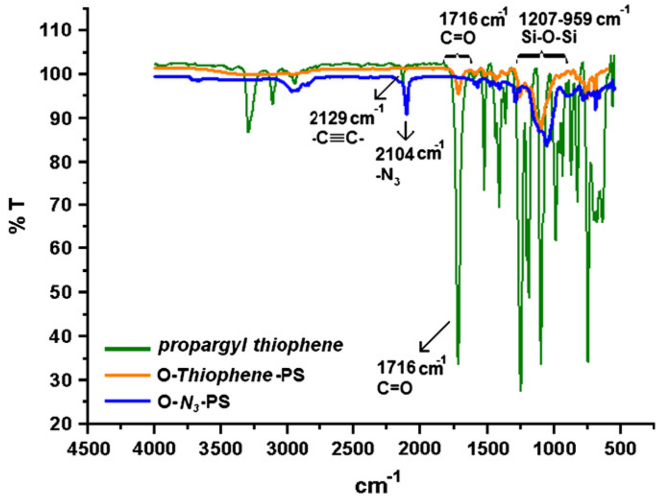

Fig. 4. FT-IR spectra of *propargyl*thiophene, O*Thiophene*PS and O*N*$_3$PS.

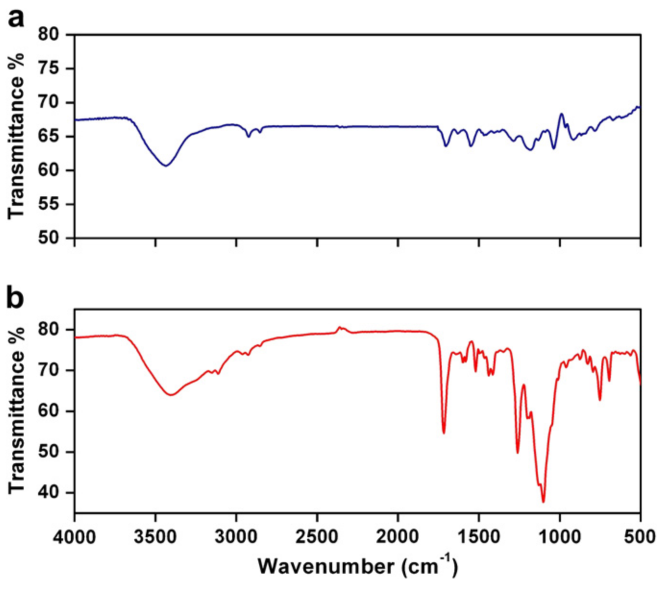

Fig. 5. FT-IR spectra of (a) OPS–PPy and (b) O*Thiophene*PS.

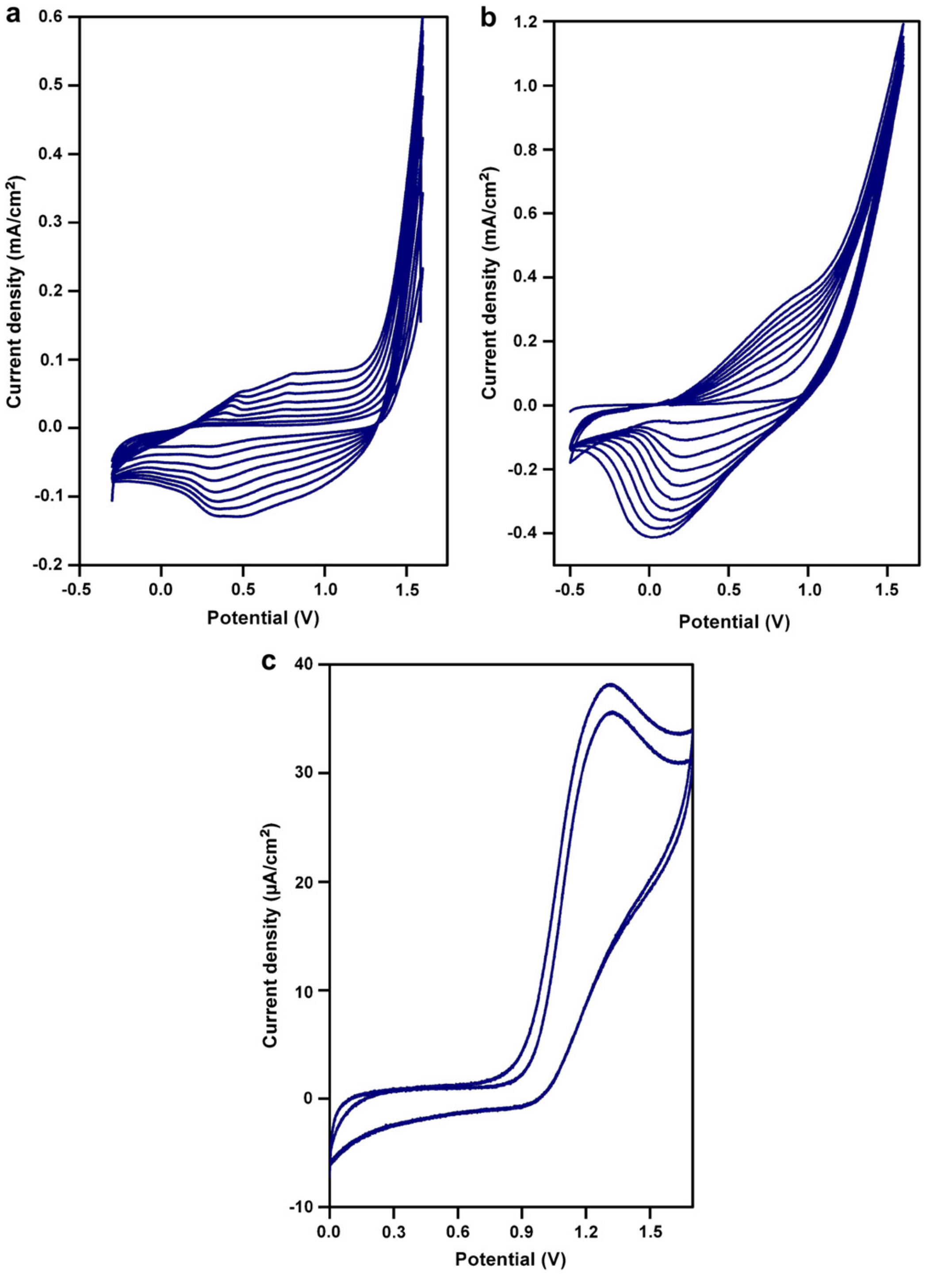

Fig. 6. Cyclic voltammograms of (a) OPS–PPy; (b) Py and (c) O*thiophene*PS.

asymmetric *ν*N–H peaks appear at 3368 cm^{-1} and 3456 cm^{-1}. After the transformation of amine groups to azide groups, a strong and new vibration centered at 2104 cm^{-1}appeared in the spectrum. Notably, all functionalized OPS, discloses characteristic of *ν*Si–O–Si stretching signals between 1304–990 cm^{-1} with relatively high intensity.

The successful transformation of azide moieties into triazole was confirmed by ^{1}H NMR. Typically, in the case of O*Thiophene*PS, the appearance of the new methylene protons adjacent to the triazole ring at 5.3 ppm (triazole–CH_2Ph) and new triazole proton at 7.8 ppm were observed (Fig. 3). Additional peaks, corresponding to thiophene moiety, overlapped with those of aromatic protons of OPS.

FT-IR spectrum of the O*Thiophene*PS (Fig. 4) reveals characteristic of *ν*Si–O–Si stretching signals between 1304 and 990 cm^{-1}. Moreover, the FT-IR spectrum also shows the disappearance of the acetylene peak at ~3293 cm^{-1} and the azide peak at ~2104 cm^{-1} while a strong carbonyl band at 1716 cm^{-1} appears. Thus, click reaction was efficient and almost quantitative as evidenced by spectral methods.

The IR spectral characteristic of O*Thiophene*PS was discussed together with that of the OPS–PPy. As seen in Fig. 5, most of the characteristic peaks of O*Thiophene*PS remained unperturbed upon electrochemical polymerization. Due to the incorporation of O*Thiophene*PS into PPy chains peak intensities in the FT-IR spectrum of OPS–PPy decreased.

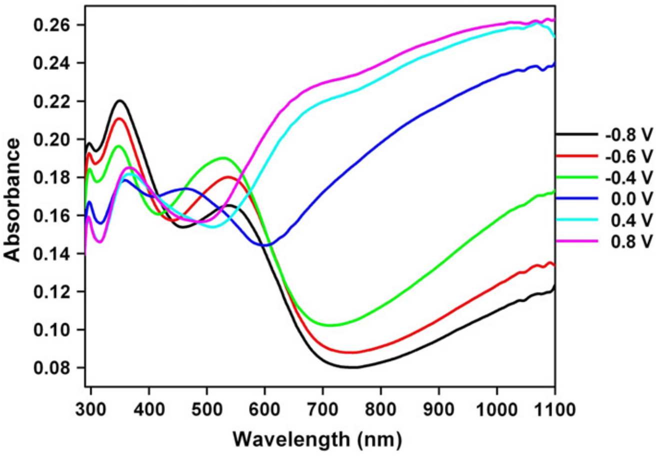

Fig. 7. Spectroelectrochemical properties of PPy in (0.1 M) DCM/TBAFB.

3.2. Cyclic voltammetry

Although O*Thiophene*PS exhibits an initial electroactivity ($E_{ox} = 1.35$ V) in TBAFB/DCM, current decreases upon repeated cycling (Fig. 6c). When CV behavior of the O*Thiophene*PS was investigated in the presence of pyrrole under same experimental conditions (Fig. 6a), there was a drastic change in the voltammogram, both the increase in the increments between consecutive cycles and the oxidation potential of the material were different from those of pyrrole (Fig. 6b), which in fact could be interpreted as the incorporation of O*Thiophene*PS in PPy chains.

Contrary to the classical polymerization, the feed ratio in conducting copolymer formation is not that important as the applied potential. This is especially true when both the two monomers in concern are electroactive. The propagation step includes the coupling of radical cations of both the monomers which is rare in classical polymerization. Compared to pyrrole the diffusion of the bulky OPS to the electrode is low. Hence, increasing the pyrrole feed results in a product where most of the properties resemble to that of the polypyrrole. On the other hand increasing the OPS content hinders the polymerization reaction. Thus, we can say that the monomer feed ratio cannot be varied in appreciable amounts. This argument is also valid if we take the following reality into account. The resulting product is the formation of polypyrrole chains in silsequioxane cores rather than a true copolymer. Thus, we can propose that the most appropriate feed ratio was selected.

The argument could have been the application of different potentials during the electrochemical polymerization. However, the activation potentials of the two monomers are quite close to each other. This means that there is no appreciable potential range to apply for. This was checked with an experiment where the potential was swept until 1.35 instead of 1.1 V and same product was obtained. On the other hand if the potential difference is too high, over oxidation problems do arise.

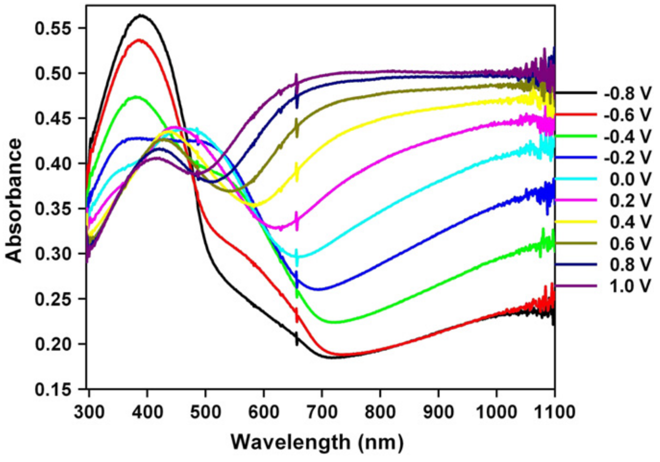

Fig. 8. Spectroelectrochemical properties of OPS–PPy in (0.1 M) DCM/TBAFB.

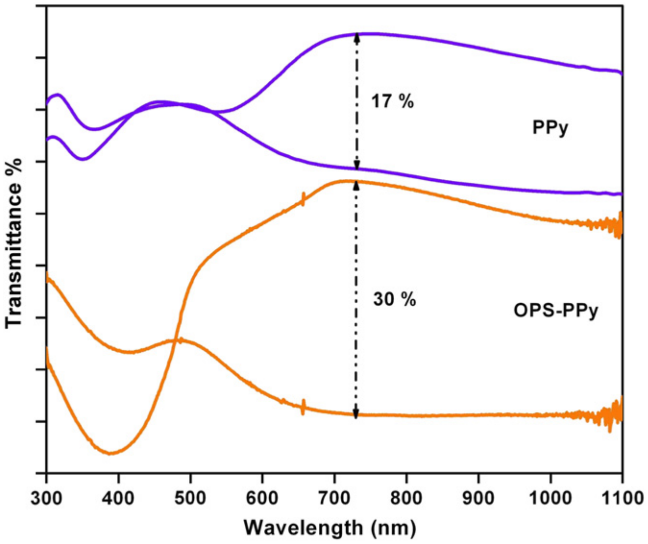

Fig. 9. Transmittance spectra of PPy and OPS–PPy in two extreme (oxidized and neutral) states.

3.3. Electrochromic properties of OPS–PPy

3.3.1. Spectroelectrochemistry

The best way of examining the changes in optical properties of conducting polymers upon voltage change is to perform spectroelectrochemistry. It also gives information about the electronic structure of the polymer such as band gap (E_g) and the intergap states that appear upon doping. OPS–PPy film was electrochemically synthesized on ITO electrode. Electrolyte solution was composed of 50 mg O*Thiophene*PS and 10 μL Py and TBAFB (0.1 M)/DCM. Increasing the pyrrole content in the feed ratio leads to a product where several properties resemble that of pyrrole, whereas increasing OPS content hinders the polymerization. In order to compare electrochromic properties, PPy and OPS–PPy were synthesized under the same electrochemical conditions. Increasing the sweep potential to +1.35 V brings no change in the electrochromic properties of the product. Spectroelectrochemical and electrochromic properties of the resultant polymers were studied by applying potentials between −0.8 V and +1.1 V in a monomer free DCM/TBAFB (0.1 M) medium. At the neutral state λ_{max} due to the π–π^* transitions for PPy (Fig. 7) and OPS–PPy (Fig. 8) were found to be 351 nm and 390 nm, respectively. Band gap of the π–π^* transitions were calculated as 2.35 for PPy and 2.25 eV for OPS–PPy. Incorporation of O*Thiophene*PS in the PPy chains gives rise to a nano-scale porous structure, where this unique molecular geometry of OPS–PPy greatly facilitates ion extraction and injection.

3.3.2. Optical contrast

Fig. 9 shows the transmittance spectra of PPy and OPS–PPy in two extreme (oxidized and neutral) states. In this study, all polymer films have approximately the same thickness as matched by chronocoulometry. By applying voltages between +1 and −1 V polymers reveal changes between colored and transmissive states. Comparison of the results shows that incorporation O*Thiophene*PS

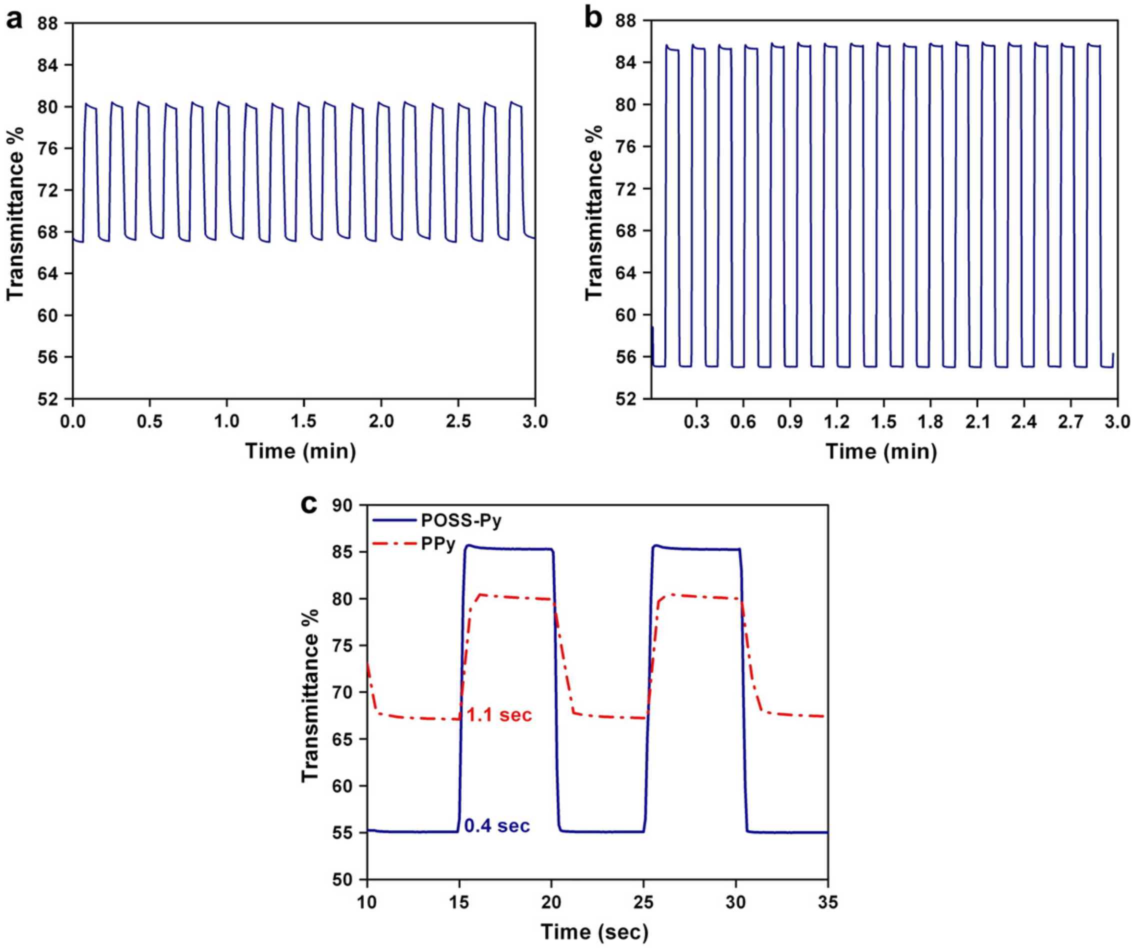

Fig. 10. Electrochromic switching, transmittance change monitored at 730 nm for (a) PPy; (b) OPS–PPy; (c) OPS–PPy and PPy (two consecutive cycles).

in PPy chains causes a noticeable increase in the optical contrast for all measured wavelengths as evidenced by an increase in the transmittance change (ΔT) from 17% to 30% (730 nm).

3.3.3. *Switching time*

Electrochromic switching studies, carried out to investigate the ability of a polymer to give a short response time, exhibit a striking color change and maintain high stability upon repeated cycles. Spectroelectrochemistry results should be taken into account in order to obtain information on the potentials to be applied for a full switch and wavelength of maximum contrast. A square-wave potential step method coupled with optical spectroscopy known as chronoabsorptometry was applied by stepping the potentials between fully oxidized and reduced states of the polymers for a residence time of 5 s during 3 min. Fig. 10a and b demonstrate the transmittance change at 730 nm for PPy and OPS–PPy examined in a repeated switching test. For comparison, we monitored the change in transmittance of a single film with the same thickness. As seen in Fig. 10c, OPS–PPy switches quite rapidly (0.4 s) compared to PPy (1.1 s). This is due to nano-porous structure of OPS–PPy facilitating ion movement during the switching.

Table 1
Electrochromic properties of OPS–PPy and PPy

Polymers	Potential (V)	Color	*L*	*a*	*b*
OPS–PPy	−1.0	Yellow	85	−5	54
	−0.5	Red	46	30	−4
	+0.2	Green-gray	45	−11	21
	+1.0	Blue	61	−25	9
PPy	−1.0	Gray	68	−10	29
	+1.0	Turquoise	58	−26	11

3.3.4. *Colorimetry*

The colors of the electrochromic materials were defined accurately by performing colorimetry measurements. CIE system was used as a quantitative scale to define and compare colors. Three attributes of color; hue (*a*), saturation (*b*) and luminance (*L*) were measured and recorded. The OPS–PPy film has distinct electrochromic properties. It shows four different colors in neutral and oxidized states. These colors and corresponding *L*, *a*, *b* values for PPy and OPS–PPy are given in Table 1.

4. Conclusion

In this study we have presented that “click chemistry” can successfully be utilized to synthesize reactive precursors for obtaining inorganic–organic conducting composites. For this purpose azide functionalized OPS was synthesized and reaction of this intermediate with *propargyl*thiophene resulted in O*Thiophene*PS. Electrochemical copolymerization of pyrrole with *OThiophene*PS was performed which resulted in star shaped polypyrrole-attached polyhedral oligomeric silsesquioxane (OPS–PPy) nanocages.

The spectroelectrochemical studies showed that the electrochromic properties of PPy such as optical contrast, switching time, color properties were greatly enhanced due to the incorporation of O*Thiophene*PS. The significant improvement is due to the loose-packed structure of OPS–PPy brought about by covalent bonding of the PPy chains to the O*Thiophene*PS cages. This star shaped novel structure greatly facilitates ion extraction and injection.

PPy-attached O*Thiophene*PS and its derivatives may find applications in multi-color electrochromism. With this approach, other polymers prepared by the copolymerization of functional O*Thiophene*PS with the wide variety of monomers may be tuned easily. The approach also provides a new platform for the development of high contrast, fast switch time and multicolored electrochromic polymers.

Acknowledgements

One of us (M. Ak) gratefully thanks DOSAP program METU.

References

[1] Imae I, Kawakami Y, Ooyama Y, Harima Y. Macromol Symp 2007;249–250:50.
[2] Xiong S, Xiao Y, Ma J, Zhang L, Lu X. Macromol Rapid Commun 2007;28:281.
[3] Skotheim TA, Elsenbaumer RL, Reynolds JR, editors. Handbook of conducting polymers. 2nd ed. New York: Marcel Dekker; 1998.
[4] Gaupp CL, Welsh DM, Rauh RD, Reynolds JR. Chem Mater 2002;14:3964.
[5] Heung CK, Kang M, Moon B, Lee H. Adv Mater 2004;16:1712.
[6] Turkaslan O, Ak M, Tanyeli C, Akhmedov IM, Toppare L. J Polym Sci Part A Polym Chem 2007;45:4496.
[7] Neves S, Santos RF, Gazotti WA, Fonseca CP. Thin Solid Films 2004;460:300.
[8] Gaupp CL, Welsh DM, Reynolds JR. Macromol Rapid Commun 2002;23:885.
[9] Krishnamoorthy K, Ambade AV, Mishra SP, Kanungo M, Contractor AQ, Kumar A. Polymer 2002;43:6465.
[10] Cecchet F, Bignozzi CA, Paolucci F, Marcaccio M. Synth Met 2006;156:27.
[11] Cho SI, Kwon WJ, Choi S-J, Kim P, Park S-A, Kim J, et al. Adv Mater 2005;17:171.
[12] Ryu JH, Lee JH, Han SJ, Suh KD. Macromol Rapid Commun 2006;27:1156.
[13] DeLongchamp D, Hammond PT. Adv Mater 2001;13:1455.
[14] Demko ZP, Sharpless KB. Angew Chem Int Ed 2002;41:2110.
[15] Kolb HC, Finn MG, Sharpless KB. Angew Chem Int Ed 2001;40:2004.
[16] Rodionov V, Fokin V, Finn MG. Angew Chem Int Ed 2005;44:2210.
[17] Helms B, Mynar JL, Hawker CJ, Frechet JMJ. J Am Chem Soc 2004;126:15020.
[18] Johnson JA, Lewis DR, Diaz DD, Finn MG, Koberstein JT, Turro NJ. J Am Chem Soc 2006;128:6564.
[19] Parrish B, Breitenkamp RB, Emrick T. J Am Chem Soc 2005;127:7404.
[20] Durmaz H, Dag A, Altintas O, Erdogan T, Hizal G, Tunca U. Macromolecules 2007;40:191.
[21] Gungor E, Cote G, Erdogan T, Durmaz H, Demirel AL, Hizal G, et al. J Polym Sci Part A Polym Chem 2007;45:1055.
[22] Altintas O, Yankul B, Hizal G, Tunca U. J Polym Sci Part A Polym Chem 2007;45:3588.
[23] Gacal B, Durmaz H, Tasdelen MA, Hizal G, Tunca U, Yagci Y, et al. Macromolecules 2006;39:5330.
[24] Ergin M, Kiskan B, Gacal B, Yagci Y. Macromolecules 2007;40:4724.
[25] Binder WH, Sachsenhofer R. Macromol Rapid Commun 2007;28:15.
[26] Lutz J-F. Angew Chem Int Ed 2007;46:1018.
[27] Kim SG, Choi J, Tamaki R, Laine RM. Polymer 2005;46:4514.
[28] Tamaki R, Tanaka Y, Asuncion MZ, Choi J, Laine RM. J Am Chem Soc 2001;123:12416.